Transilvania University of Brasov
FACULTY OF MECHANICAL ENGINEERING

ICMS 2019 & COMEC 2019
Brasov, ROMANIA, 21-22 November 2019

ON THE EIGENVALUE TORSIONAL BUCKLING BY FINITE ELEMENT ANALYSIS OF CFRP COMPOSITE SHAFTS SUBJECTED TO TORQUE WITH AN IMPOSED TRANSVERSAL DISPLACEMENT

Marius Nicolae Baba[1], Levente Józsa[1], Christos Potamitis[2]
[1] Transilvania University of Brașov, Brașov, ROMANIA, mariusbaba@unitbv.ro; levente.jozsa@student.unitbv.ro
[2] University of West Attica, Athens, GREECE, xristos.potamitis@gmail.com

Abstract: *In this paper, a FE computational model based on the eigenvalue procedure was developed to predict the torsional buckling capacity of CFRP shafts. The FE model was validated based on a detailed convergence study as well as against experimental results reported in literature for five particular composite shaft's configurations. Several valuable recommendations related to the size and type of finite elements along with the appropriate application of boundary conditions to properly simulate the constraints at the supporting ends are provided. To investigate the influence of unavoidable imperfections of support settlements on torsional stability behavior of CFRP shafts, the FE model was updated by imposing a transverse displacement to the torque moment application end-point. Some quantitative results of torque capacity decrement relative to the fiber orientation and stacking sequence for the particular shaft's configurations in question are also reported.*
Keywords: *CFRP shaft, FEA, eigenvalue torsional buckling, layup orientation, critical buckling torque, imperfection*

1. INTRODUCTION

Nowadays the use of CFRP drive shafts within a variety of industrial fields is becoming increasingly common due to their weight saving potential relative to conventional metallic materials. As the main part of any power transmission system, their use in the near future is expected to widely extend from the automotive and aerospace applications toward some other highly specialized engineering fields such as the development of lightweight rotating machinery for onshore/offshore wind turbine generators.
Since the CFRP shafts are relatively lighter and less stiff, their torsional buckling capacity is essential when carrying various combinations of in-service operating loads. Moreover, as in the real engineering practice the loads are often applied with an offset and the supports are never perfectly rigid, the preload-induced stresses are likely to occur and inherently lead to the change of stiffness of composite shafts. Thus, the load-carrying capacity of drive shafts made of carbon fiber reinforced composite laminates may reduce significantly due the imperfect settlements of supports. In a such a context, a further extension of the use of carbon-reinforced laminate shafts in large-scale engineering applications by developing reliable lightweight power transmission systems still necessitate considerable research efforts to analyze and prevent the loss of stiffness induced damages as well as the catastrophic failures due to torsional buckling.
Bachau et al. [1], compared the experimental measured torsional buckling of Graphite/Epoxy shafts with the theoretical predictions relied on a general shell theory that includes the elastic coupling effects as well as the transverse shearing deformations. They found that the direction of the applied torque along with the layup stacking sequence greatly affects the torsional buckling capacity of thin-walled laminate Graphite/Epoxy shafts and furthermore, their torsional response is more related to the stiffness characteristics rather than the material strength.
Based on a complex theoretical analysis, Bert and Kim [2], predicated the torsional buckling load of composite drive shafts with various layups by considering the effect of off-axis stiffness under pure torque loading and also the combined loading of torsion with bending.
Mahmood et al. [3], reviewed the closed form solution methods to calculate the buckling torque of composite drive shafts and compared the results of eigenvalue torsional buckling FEA studies with the experimental and analytical data provided by [1] and [2]. They showed a better agreement between the FEA and experimental results compared with the analytical methods. However, they did not provide valuable recommendations neither about the suitable size of finite element mesh used to obtain the appropriate solution nor about the way, the physical applied torque as well as the shaft fixed-end boundary conditions were implemented in the finite element model.
A number of other authors have addressed the problem of torsional buckling of composite shafts by analytical,

experiments and/or finite element analysis [4], [5], [6], [7] and [8]. The analysis of Cherniaev and Komarov [9] is particularly relevant since the design of Carbon/Epoxy drive shafts is approached as a multistep optimization process. It essentially includes the following three steps: 1) determination of fiber orientation and the laminate stacking sequence based on the analysis of loading conditions, the analytical expressions predicting buckling load as well as the minimal natural frequency of idealized drive shaft model; 2) finding the rational ply thicknesses using a formal optimization procedure using the response surface approximations along with the gradient-based optimization algorithm; and 3) verification of the optimized configuration with the use of nonlinear buckling analysis to ensure that the stability constraints are satisfied. However, neither specifications about the appropriate modeling of unavoidable imperfections of support settlements nor their influence on torsional load-bearing buckling capacity of CFRP shafts are provided.

The overall objective of the current paper is to present a brief calculation guideline of CFRP shafts torsional buckling capacity by means of eigenvalue FE analysis. The obtained critical buckling torques for several geometric and stacking configurations are compared with the existent experimental data from literature to establish the appropriate finite element type and size as well as the constraints against which the ends of the shaft are prescribed to properly approximate the physical reality. The approach could be then used for advanced parametric design studies in such a way that only a few FE computations would be necessary to evaluate the critical buckling torque due to the deformations during operation, misalignment of bearings supports or incorrect tolerances for press fits of bearings; that all may lead to transverse displacements of driving shaft. Some quantitative results for torque capacity decrement relative to the fiber orientation and stacking sequence for the particular shaft's configurations in question are also provided.

Hereinafter, we shall restrict our discussion to CFRP shafts that lose their stability by bifurcation (torsional buckling) assuming that the dynamic character of the load is not taken into account, the stresses and strains do not exceed the elastic material range and the deformations are small. The term bifurcation refers to the buckling onset, which is predicted by FE analysis [10], [11]. That is, at the critical buckling load, on the load-deflection curve the displacements begin to grow in a new pattern that is different with respect to the pre-buckling fashion.

2. RESEARCH METODOLOGY

For the current work, a FE computational model based on the eigenvalue buckling procedure was adopted through a comparative study related to the size and type of finite elements as well as the appropriate application of boundary conditions to properly simulate the constraints at the supporting ends. The FE model was then validated against the experimental data reported by Bachau et al. [1]. To investigate the influence of unavoidable imperfections of support settlements on torsional stability behavior of CFRP shafts, the FE model was updated by imposing a transverse displacement to the torque moment application end-point. In such a context, the eigenvalue torsional buckling analysis is preceded by a linear static analysis to determine the pre-bucking stress field corresponding to the imposed transverse displacement at the shaft's torque loading end-point. The results are then used in the neutral equilibrium condition when solving the eigenvalue buckling problem.

2.1. Description of FEA model

Commercial software Abaqus/CAE was used in this study to perform the eigenvalue buckling calculations. Five particular CFRP shaft's configurations (see Table 1) taken from the reference literature [1], were considered in the FE analysis.

Table 1: The CFRP shafts stacking layup and geometry

The CFRP shaft configuration nomenclature	The laminate stacking layup.	The shaft mean radius, R [mm]	The shaft length, L [mm]
M1	15/-15/-45/-15/15/45	41.27	260
M2	-45/-15/15/45/15/-15	41.27	260
M3	30/-30/30/-30/30/-30	37.19	320
M4	45/-45/45/-45/45/-45	37.42	320
M5	0/0/45/-45/45/-45/0/0	37.42	320

As reported by Bachau et al [1], circular cylindrical specimens were fabricated from 6 or 8 layers of prepreg wrapped around an aluminum mandrel. The prepreg consists of Union Carbide's T300 graphite fibers in Fiberite's

948Al low temperature curing epoxy. The elastic properties of composite laminae and the layer thickness that were considered in the FE based calculations are reported in Table 2 [1].

Table 2: The mechanical properties and layer thickness of composite lamina

$E_L = E_1$ [MPa]	$E_T = E_2$ [MPa]	$G_{LT} = G_{12}$ [MPa]	$G_{LR} = G_{13}$ [MPa]	$G_{TR} = E_{23}$ [MPa]	$\nu_{LT} = \nu_{12}$ [-]	Layer thickness [mm]
134000	8500	4600	4600	4000	0.29	0.334

The composite shaft is fixed at one end subjected to a unit torque couple at the other end. Figure 1 shows the shaft geometry and FE model. It also shows a detailed view of the way, the constraints definition are applied to prescribe the displacements and rotations at the shaft-loaded end. As highlighted in the figure, the center point is the reference point while the perimeter nodes are the slave nodes. Referring to the slave nodes, for a proper idealization of the physical bearing constraints at the shaft ends, two types of constraint definitions (spider connection elements) were considered to a comparative analysis, as presented in Table 3.

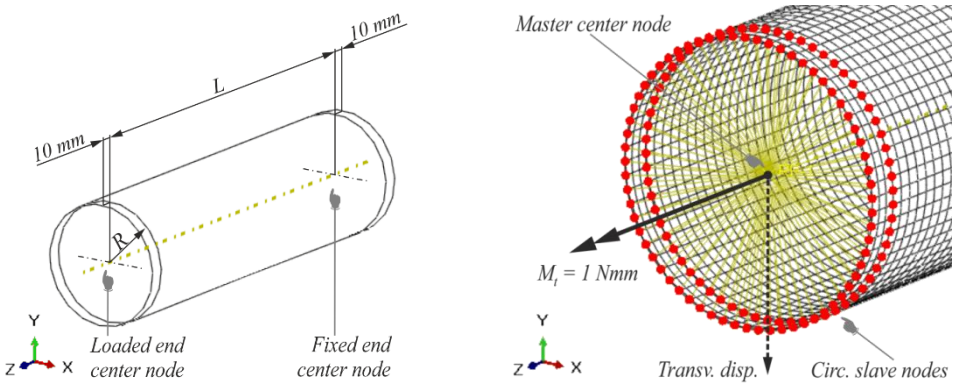

a) Isometric view of CFRP shaft geometry b) Detailed FEM of CFRP shaft-loaded end

Figure 1: CFRP shaft geometry and FEM

With reference to Table 3, it has to be noted that the specified degrees of freedom are related the global coordinate system shown in Figure 1.

Table 3: Configurations of CFRP shaft model end constraints

The nomenclature and definition of boundary conditions	Clamped at both ends	Pined at both ends without axial constraint
Abaqus/CAE typical constraints definition	**Constraint: *MPC BEAM	**Constraint: *Kinematic 1,1 2,2
Slave nodes inactive DOFs with respect to global coordinate system (see Figure 1)	UX, UY, UZ, RX, RY, RZ	UX, UY

As concern the effects of boundary conditions, they have to be considered relative to the spider connection elements used to idealize the physical bearing constraints at the shaft ends. In this regard, based on a detailed comparative FE study (see Figure 2), it was found that the use of Abaqus standard kinematic constraints with two selected translational degrees of freedom, corresponding to blocked linear displacements within the cross-sectional planes of the shaft, led to the best fit with the existing experimental data from literature. In order to avoid the over-stiffening effects, these shaft-end kinematic constraints (spider connection elements) were applied selectively in such a way that they follow a particular pattern made of only two rows of circumference nodes with a gap distance of 10 mm measured from both end edges.

The performances of three Abaqus general-purpose shell elements (S4: linear elements, S4R: linear elements with reduced integration 1x1 and S8R: second order parametric elements S8R with reduced integration 2x2), were assessed based on a convergence study with the corresponding experimental results from literature. Figure 2 show

the results of convergence study related to the applied boundary conditions as well as the shell element size and type versus critical buckling torque moment as well as the corresponding CPU time ratio.

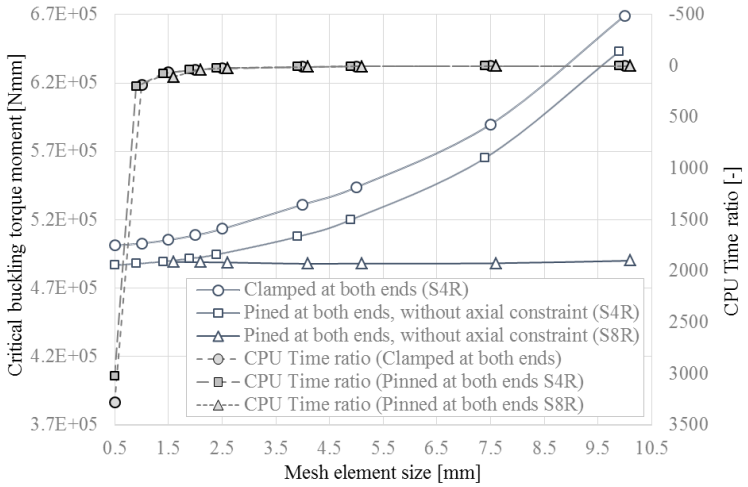

Figure 2: The FE convergence curve of critical buckling torque versus CPU time ratio

One may easily conclude that relative to CPU time ratio, the FE mesh build-up by doubly curved shell elements, reduced integration, S8R, with the size of 4 mm are providing the most reasonable convergence.

2.2. Validation of FEA results for the base model (with no imposed transverse displacement)

The accuracy of results obtained based on the aforementioned FEA models (with no any imposed transversal displacement) have been check against the experimental data reported by Bauchau et al [1] as listed in Table 4. For comparison purposes the FEA results obtained by Mahmood M et al. [3] are also presented in the same table.

Table 4: Comparisons of critical buckling torque results

The layup model of CFRP shaft	The critical buckling torque moment [Nmm]			
	Experimental results data, Ref. [1]	FEA results data, Ref. [3]	Results of actual FEA based models	
			S4R, clamped ends: 1.5 mm elm. size	S8R, pinned ends w/o axial constraint: 4 mm elm. size
M1: 15/-15/-45/-15/15/45	486000	472000 (-3%)	505227 (4%)	487859 (0.4%)
M2: -45/-15/15/45/15/-15	350000	372000 (6%)	401302 (15%)	387645 (11%)
M3: 30/-30/30/-30/30/-30	390000	395000 (1%)	439041 (13%)	418366 (7%)
M4: 45/-45/45/-45/45/-45	490000	460000 (-6%)	533844 (9%)	504970 (3%)
M5: 0/0/45/-45/45/-45/0/0	543000	670000 (23%)	668180 (23%)	630279 (16%)

In the above table, the value between parentheses represent the calculated percent deviations from the experimental data. One may observe that the results obtained based on the model pinned at both ends without axial constraint, meshed with doubly curved shell elements with reduced integration S8R (4 mm element sixe), fit better the experimental results compared to the others.

3. RESULTS AND DISCUSSIONS

The same as modal frequencies in the modal analysis, the buckling load factors are converging from above. Being also already known from literature, the eigenvalue buckling analysis allows to determine only the upper limit of torsional buckling capacity and, as the results reported in this paper show, in cases of present composite shaft's configurations subjected to torque it is overestimated with a maximum deviation of 16% referring to the experimental data (see Table 4), thus leading to non-conservative results. In such a context, considering also the discretization and modeling errors, the results of eigenvalue buckling analysis must be interpreted with caution.
Figure 3 depicts the deformation states corresponding to the results of eigenvalue buckling analyses steps without and with 5 mm imposed transverse displacement.

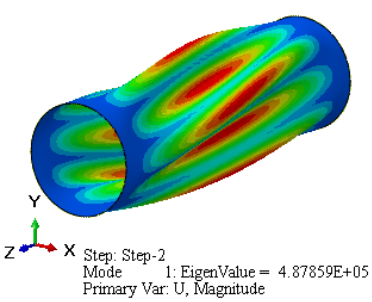

a) M1: 15/-15/-45/-15/15/45; 1st eigenvalue (torque)

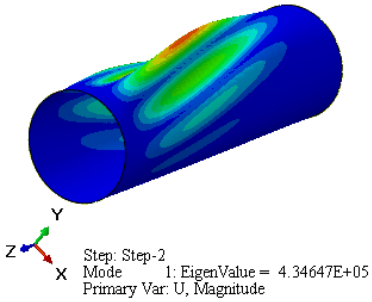

b) M1: 1st eigenvalue (torque + 5 mm transv. disp.)

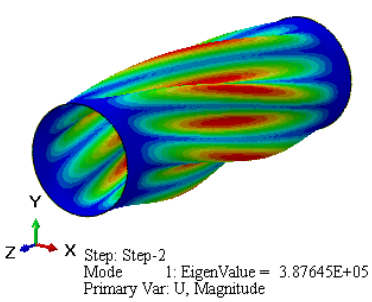

c) M2: -45/-15/15/45/15/-15; 1st eigenvalue (torque)

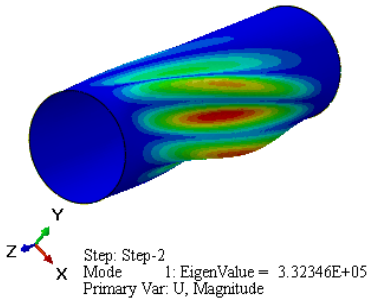

d) M2: 1st eigenvalue (torque + 5 mm transv. disp.)

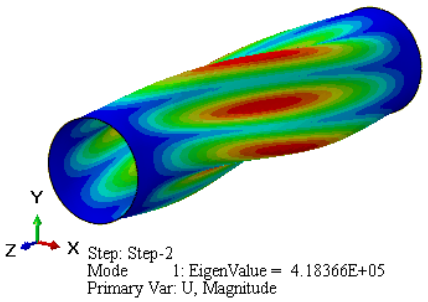

e) M3: 30/-30/30/-30/30/-30; 1st eigenvalue (torque)

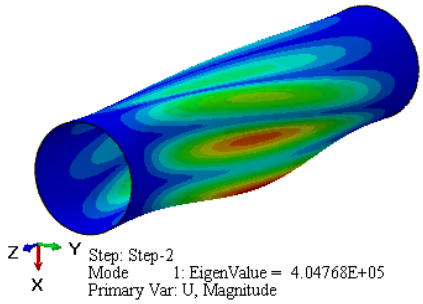

f) M3: 1st eigenvalue (torque + 5 mm transv. disp.)

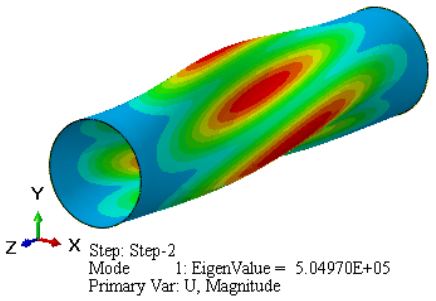

g) M4: 45/-45/45/-45/45/-45; 1st eigenvalue (torque)

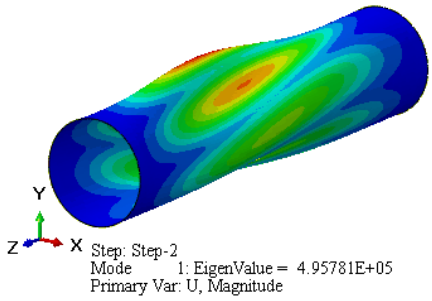

h) M4: 1st eigenvalue (torque + 5 mm transv. disp.)

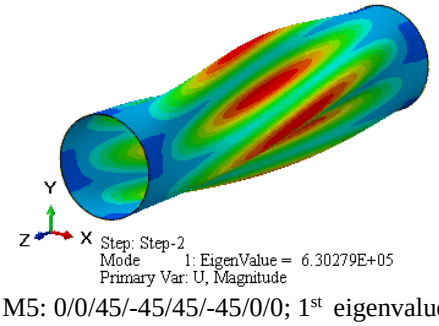

i) M5: 0/0/45/-45/45/-45/0/0; 1st eigenvalue (torque)

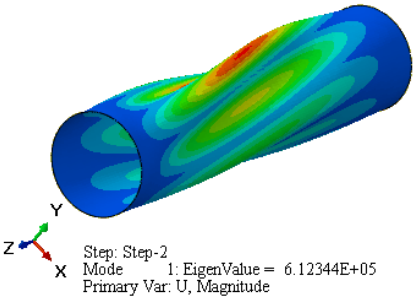

j) M5: 1st eigenvalue (torque + 5 mm transv. disp.)

Figure 3: The deformation states corresponding to eigenvalue buckling analyses steps without and with 5 mm imposed transversal displacement

Only the lowest eigenvalues (load multipliers) and the corresponding buckling modes are represented in the above figure as they are of interest. As the buckling mode shapes are normalized vectors so that the maximum displacement has a unitary magnitude, they do not represent the actual deformation magnitudes at the critical load. However, the buckling mode shapes are useful qualitative indicators in the eigenvalue torsional buckling analysis, since they likely predict the appropriate failure modes.
The decrement of critical buckling torque moment relative to increase of the imposed transverse displacement between 0 to 5 mm, is plotted in Figure 4.

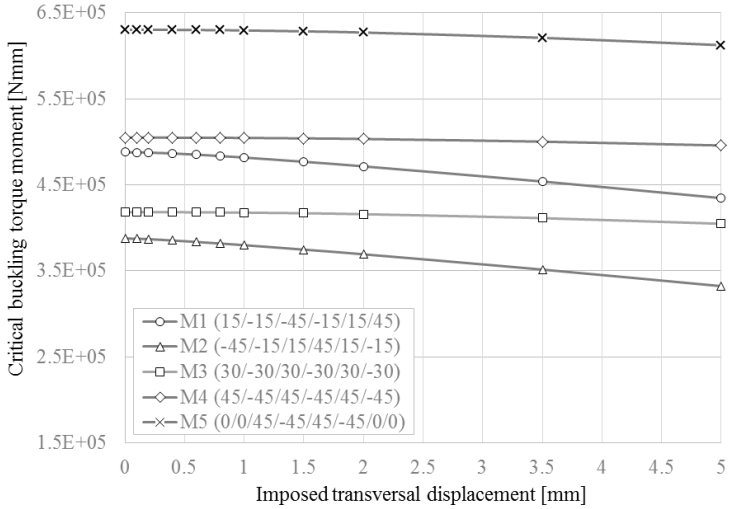

Figure 4: The critical buckling torque decrement with increase of the imposed displacement

The plot in the figure above shows that the most sensitive stacking layout when preloading with an imposed transverse displacement at the loaded end is 15/-15/-45/-15/15/45, as it actually leads to a decrement of buckling load factor equal to 11%. On the other side, the less sensitive stacking layout is 45/-45/45/-45/45/-45, leading to a buckling load factor decrement of 2%.

4. CONCLUSIONS

A finite element study was developed to predict the eigenvalue torsional buckling of CFRP shafts. The problem of shaft torsional stability by bifurcation is sensitive on the size and type of finite elements as well as the modeling of boundary conditions in conjunction with the spider connection elements (kinematic constraints) used to idealize the physical bearing constraints at the shaft ends.
To avoid the over-stiffening effects, the application of kinematic constraints (spider connection elements) to pin the shaft at both ends without axial constraint leads to a good agreement of FE results with experimental data. However, these spider elements have to be applied selectively in such a way that they follow a particular pattern made of only two rows of circumference nodes at each shaft end.
Relative to CPU time, the results obtained using doubly curved shell elements S8R with the size of 4 mm were provided the best fit to the experimental data.
The modelling of preload-induced stress imperfections due to various factors such as machine deformation during operation, misalignment of bearings supports or incorrect tolerances for press fits of bearings; must be considered when evaluating the critical buckling torque capacity of CFRP shafts. Of the shaft's configurations under analysis by eigenvalue buckling FE-based computation, the most sensitive stacking layout when preloading with an imposed transverse displacement at the loaded end is 15/-15/-45/-15/15/45, as it actually leads to a decrement of buckling load factor equal to 11%. On the other side, the less sensitive stacking layout is 45/-45/45/-45/45/-45, leading to a buckling load factor decrement of 2%.
As the buckling load factor is typically overestimated, thus leading to non-conservative results, and considering also the discretization and modeling errors, the results of eigenvalue buckling analysis must be interpreted with caution. However, since it provides a quite reasonable estimation of the torsional buckling load factor and requires a relatively low computational time, during the preliminary design phases a scale-down factor of 1.3 may be conservatively applied to correct the FE-based calculated eigenvalue critical buckling torque. Future work shall

be focused towards the validation of this proposal by nonlinear FE computations and extended analysis of experimental data.

REFERENCES

[1] Bauchau OA, Krafchack TM and Hayes JF (1988) Torsional buckling analysis and damage tolerance of graphite/epoxy shaft. J Compos Mater 1988; 22:258–70.

[2] Bert CW and Kim CD (1995) Analysis of buckling hollow laminated composite drive shafts. Compos Sci Technol 1995; 53:343–51.

[3] Mahmood M, Shokrieh Akbar Hasami and Larry B. Lessard (2004) Shear buckling of composite drive shafts under torsion. Composite Structures. 64 (2004) 63–69.

[4] Mutasher SA. Prediction of the torsional strength of the hybrid aluminum/ composite drive shaft. Mater Des 2009;30 (2):215–20.

[5] Abu Talib AR, Ali A, Badie MA, Lah NA, Golestaneh AF. Developing a hybrid, carbon/glass fiber-reinforced, epoxy composite automotive drive shaft. Materials and Design 31 (2010) 514–521.

[6] Montagnier O and Hochard Ch (2016) Optimisation of hybrid high-modulus / high-strength carbon fiber reinforced plastic composite drive shafts. Materials and Design 46 (2016) 88-100.

[7] A. Khalkhali A, Nikghalbb E and Norouzianc M (2015) Multi-objective Optimization of Hybrid Carbon/Glass Fiber Reinforced Epoxy Composite Automotive Drive Shaft. IJE TRANSACTIONS A: Basics Vol. 28, No. 4, (April 2015) 583-592.

[8] Cinar K, Nuri Ersoy N and Akif Unal M (2018) Design of a real-sized composite drive shaft and the critical points from begining to end. ECCM18 - 18th European Conference on Composite Materials, Athens, Greece, 24-28th June 2018.

[9] Cherniaev A and Komarov V (2015) Multistep Optimization of Composite Drive Shaft Subject to Strength, Buckling, Vibration and Manufacturing Constraints. Appl Compos Mater (2015) 22: 475–487.

[10] Sun BH, Yeh KY and Rimrott FPJ (1995) On the Buckling of Structures. Technische Mecahnik (44) (1995) 129-140.

[11] Vlase S, Marin M and Öchsner A (2019) Eigenvalue and Eigenvector Problems in Applied Mechanics. Springer Nature Switzerland AG, 2019.